

## Self-consistent static-density-response function of a metal surface in density-functional theory

Adolfo G. Eguiluz

*Department of Physics, University of California at Irvine, Irvine, California 92717*

(Received 30 October 1984)

We obtain the static-linear-density-response function of the conduction electrons in a metal slab in a self-consistent-field approximation derived from density-functional theory. Exchange and correlation effects are included within the local-density-functional (LDF) approximation. The jellium model is used for the periodic ionic background. The response function is obtained by solving a matrix equation for the coefficients of a double-cosine Fourier-series representation for the response. Our solution holds for all values of the two-dimensional wave-vector transfer parallel to the surface  $q_{\parallel}$ . The entire surface-screening problem is basically reduced to carrying out matrix algebra on the computer. Our method provides a good approximation for the response function of a semi-infinite medium. We test the method by computing the electron density induced by an impurity placed in the surface region. The singularity of the response function for  $q_{\parallel}=2k_F$  ( $k_F$  being the Fermi wave vector) gives rise to long-range lateral oscillations in the induced density. The amplitude of these oscillations becomes vanishingly small when the impurity is placed outside the jellium. The oscillations in the induced density along the surface normal are also studied. We quantify the importance of exchange and correlation effects in the response function by comparing the results obtained in the LDF and random-phase approximations.

### I. INTRODUCTION

An accurate description of screening at a metal surface is essential for the quantitative study of, e.g., pair potentials between ions belonging to the outer atomic layers,<sup>1,2</sup> lateral interactions between adsorbed atoms<sup>3,4</sup> (which determine the geometry of an adsorbed layer of atoms), and for the microscopic theory of lattice dynamics of clean and adsorbate-covered metal surfaces.<sup>5,6</sup> A basic element of the physics of these problems is the screening response of the conduction electrons to a local charge imbalance. It is this question to which the present paper is devoted.

Surface screening of an impurity including the effects of electron-electron interactions through the use of the random-phase-approximation (RPA) linear-density-response function of the electron gas has been considered by several authors.<sup>1,2,7-12</sup> However, in all of this work the rather drastic step is taken of assuming that in the ground state the electrons are noninteracting, being confined solely by an infinite potential wall placed at a distance  $z_0=3\pi/8k_F$  from the jellium edge. This is the infinite-barrier model (IBM), first considered by Bardeen many years ago.<sup>13</sup> Sometimes the additional simplifying assumption is made of neglecting the "quantum-interference terms" in the response function.<sup>7-11,14</sup> This is the classical infinite-barrier model, in which the electron-density profile at the surface has a step discontinuity.

Now, the importance of self-consistency in the electron density profile and effective potential used in the study of surface electronic properties is well established.<sup>15,16</sup> Furthermore, in the present context of surface-impurity screening, recent results of Rasolt and Perrot,<sup>1</sup> obtained using the IBM for the electron wave functions, suggest

the importance of including exchange and correlation effects in the surface response function. For example, they give rise to a sizable shift in the position of the effective image plane relative to the value obtained in the RPA.<sup>17</sup> It is clear that further progress in the quantitative study of surface screening requires the use of a surface-response function that incorporates the electron-electron interaction self-consistently. By this we mean that the same treatment of the electron-electron interaction that goes in the computation of the response should go in the computation of the ground-state electron-density profile and surface potential. This is done in the present paper. We obtain the static-linear-density-response function for a jellium surface in a self-consistent-field approximation derived from density functional theory.<sup>18</sup> Exchange and correlation effects are included within the local-density-functional (LDF) approximation for the exchange and correlation functional.<sup>18</sup> The Lang-Kohn electron density profile at the surface is used.<sup>15</sup>

In the case of bulk screening it has been known for many years<sup>19</sup> that the electron density induced by an isolated impurity embedded in an otherwise uniform electron gas has the asymptotic form

$$n_{\text{ind}}(r) \rightarrow r^{-3} \cos(2k_F r), \quad (1.1)$$

for  $k_F r \gg 1$ , where  $r$  is the radial distance from the impurity. Equation (1.1) is a direct consequence of the logarithmic singularity of the bulk density response function at  $2k_F$ .<sup>19</sup> Experimental evidence for the long-range Friedel oscillations (1.1) is found in studies of the Knight shift and quadrupolar broadening of the nuclear magnetic resonance line of the solvent atoms in dilute alloys.<sup>20</sup>

A conceptually important paper on the subject of sur-

face screening is Lau and Kohn's paper<sup>4</sup> on the indirect long-range interaction between a pair of adsorbed atoms. Lau and Kohn<sup>4</sup> effectively proved that the surface response function for noninteracting electrons has a weak singularity for  $q_{\parallel}=2k_F$  (the leading singular term is of the form  $|q_{\parallel}-2k_F|^{7/2}$ ). From this result these authors proved the existence of a long-range oscillatory contribution to the indirect lateral interaction between the two atoms (the oscillation has period  $\pi/k_F$  and it decays asymptotically like the fifth power of the lateral distance between the charges). From the structure of the integral equation that we solve in Sec. II it follows that the full-response function (i.e., the response function in the presence of electron-electron interactions) has a similar singular behavior for  $q_{\parallel}=2k_F$  as the response function for noninteracting electrons. One virtue of our formulation is that this weak singularity of the response function is easily handled numerically.

The outline of this paper is as follows. In Sec. II we obtain and solve the integral equation for the static density response function of a jellium slab in the LDF approximation. Although our method makes essential use of the assumption of a finite slab thickness, in practice it turns out to give a good approximation to the response of a semi-infinite medium for rather small thicknesses. Our solution comes in the form of a matrix of coefficients of a double-cosine Fourier series representation for the response function. That matrix is obtained solving a matrix equation numerically. The entire surface-response problem is reduced to carrying out matrix algebra on the computer by using a simple (sine-) series representation for the self-consistent electron wave functions. Our solution for the response holds for all values of the two-dimensional wave-vector transfer parallel to the surface. This is an important point, since in the screening of a surface impurity, small-wave-vector expansions are inadequate. We note that Dobson and Harris<sup>21</sup> have recently given an entirely numerical solution to the same integral equation considered in Sec. II. Their approach to the study of surface response would require the tabulation of the response function over a double mesh of values of the coordinate normal to the surface. The method put forth in the present paper appears to be easier to implement. As an illustration, in Sec. III we address a basic screening property: We compute the electron density induced by a point-charged impurity located near the surface. We place emphasis on the long-range oscillations in the induced density both in directions parallel and normal to the surface. We examine the effect of the proximity of the surface on the long-range behavior. The Appendix is dedicated to the study of the density response function for noninteracting electrons. This response function enters the kernel of the integral equation solved in Sec. II. In this Appendix we find it convenient to consider the dynamical response first, and obtain the required static response as the zero-frequency limit of the former. We thus take the opportunity to provide the derivation of the result for the dynamical response function for noninteracting electrons used in a recent paper.<sup>22</sup>

There are three main approximations used in this paper. (i) We use the jellium model for the periodic ionic back-

ground. This assumption is introduced in the computation of the response function. Thus our results apply only to simple (*s-p*-bonded) metals such as aluminum and the alkalis. However, more complicated metal surfaces also contain a large contribution to the response from the *s-p* electrons. (ii) Exchange and correlation effects are included within the local-density approximation.<sup>18</sup> Gunnarsson and Lundqvist have given an appealing qualitative justification for this approximation,<sup>23</sup> which has been shown to give good results for the electron-density profile and total energies in the metal-surface problem.<sup>23</sup> (iii) Our formulation is based on the use of the *linear* density response function of the conduction electrons. Now, this response function is currently being used in the study of lattice-dynamical properties of simple metal surfaces in the harmonic approximation.<sup>24</sup> In that case, the linear electronic response is all that is needed.<sup>5</sup> On the other hand, if what is required is an accurate value of, say, the charge build-up at the position of a point impurity, then one should probably resort to other formulations<sup>25</sup> that do not require the assumption of linearity in the response. We would like to note that a paper by Appelbaum and Hamann<sup>26</sup> gives support to the use of a linear theory in some surface calculations. Using a variational method, these authors found that the interaction energy between a point charge of magnitude  $Q$  and a jellium surface, scales as  $Q^2$  for values of  $Q$  up to  $2e$  ( $e$  being the magnitude of the electron charge) and for impurity-jellium separations down to 1 a.u. Lang and Williams<sup>25</sup> and Gunnarsson and Hjelmberg<sup>25</sup> have criticized the linear approximation in the context of the theory of chemisorption, as have Almlath *et al.*<sup>27</sup> in the case of a proton in a bulk metal. However, it would be straightforward to use a pseudo-ion instead of a point impurity<sup>1</sup> (i.e., an impurity with an appropriate finite core size). It is expected that the error due to the linear approximation should decrease with the size of the core.

## II. DENSITY-RESPONSE FUNCTION IN THE LDF APPROXIMATION

### A. Integral equation for the response function

The static-density-response function  $\chi(\mathbf{x}, \mathbf{x}')$  is defined by the equation

$$n_{\text{ind}}(\mathbf{x}) = \int d^3x' \chi(\mathbf{x}, \mathbf{x}') U_{\text{ext}}(\mathbf{x}'). \quad (2.1)$$

where  $n_{\text{ind}}$  is the electron number density induced by an external potential  $U_{\text{ext}}$ . The integral in Eq. (2.1) runs over the metal interior.

In a self-consistent-field theory one also introduces a response function for noninteracting electrons,  $\chi^{(0)}(\mathbf{x}, \mathbf{x}')$ , defined by the equation

$$n_{\text{ind}}(\mathbf{x}) = \int d^3x' \chi^{(0)}(\mathbf{x}, \mathbf{x}') U_{\text{sc}}(\mathbf{x}'), \quad (2.2)$$

where

$$U_{\text{sc}}(\mathbf{x}) \equiv U_{\text{ext}}(\mathbf{x}) + U_{\text{ind}}(\mathbf{x}). \quad (2.3)$$

In Eq. (2.3) we have introduced the potential  $U_{\text{ind}}(\mathbf{x})$  giving the average field acting on an electron as a conse-

quence of the screening response of the electron system to the external field [which gives rise to the induced-charge density  $-en_{\text{ind}}(\mathbf{x})$ ]. In density-functional theory,<sup>18</sup>  $U_{\text{ind}}(\mathbf{x})$  is obtained by linearizing the change of the effective potential  $V_{\text{eff}}(\mathbf{x})$  in which the electrons move [the effective potential of the Kohn-Sham equation (A2)]. In the local-density-functional (LDF) approximation for the exchange and correlation potential  $V_{\text{xc}}(\mathbf{x})$  [cf. Eq. (A3)], we have<sup>28,29</sup>

$$U_{\text{ind}}(\mathbf{x}) = e^2 \int d^3x' \frac{n_{\text{ind}}(\mathbf{x}')}{|\mathbf{x} - \mathbf{x}'|} + \frac{dV_{\text{xc}}(\mathbf{x})}{dn_0(\mathbf{x})} n_{\text{ind}}(\mathbf{x}), \quad (2.4)$$

where  $n_0(\mathbf{x})$  denotes the electron number density in the ground state of the unperturbed system (i.e., in the absence of the impurity).

From Eqs. (2.1)–(2.4) it is a simple exercise to establish an integral equation for  $\chi(\mathbf{x}, \mathbf{x}')$ . We have<sup>21,28</sup>

$$\begin{aligned} \chi(\mathbf{x}, \mathbf{x}') &= \chi^{(0)}(\mathbf{x}, \mathbf{x}') \\ &+ \int d^3x_1 \int d^3x_2 \chi^{(0)}(\mathbf{x}, \mathbf{x}_1) V(\mathbf{x}_1, \mathbf{x}_2) \chi(\mathbf{x}_2, \mathbf{x}'), \end{aligned} \quad (2.5)$$

where  $V(\mathbf{x}_1, \mathbf{x}_2)$ , the full electron-electron interaction in the LDF approximation, is given by the equation

$$V(\mathbf{x}_1, \mathbf{x}_2) = \frac{e^2}{|\mathbf{x}_1 - \mathbf{x}_2|} + \frac{dV_{\text{xc}}(\mathbf{x})}{dn_0(\mathbf{x})} \delta(\mathbf{x}_1 - \mathbf{x}_2). \quad (2.6)$$

The integral equation (2.5) has the simple diagrammatic interpretation shown in Fig. 1. The noninteracting electron-response function  $\chi^{(0)}(\mathbf{x}, \mathbf{x}')$  is given by the electron-hole bubble (or the RPA approximation for the irreducible response). For convenience in the presentation  $\chi^{(0)}(\mathbf{x}, \mathbf{x}')$  is analyzed in detail in the Appendix. The dashed lines represent the full interaction  $V(\mathbf{x}_1, \mathbf{x}_2)$ . Iteration of Eq. (2.5) yields the geometric series represented in Fig. 1, whose  $(n + 1)$ th term is of  $O(V^n)$ .

The conceptual simplicity of the LDF integral equation (2.5) stems from the fact that exchange and correlation are included in the interaction  $V(\mathbf{x}_1, \mathbf{x}_2)$  [and only through a simple function of  $n_0(\mathbf{x})$ ], while the irreducible response  $\chi^{(0)}$  is that for noninteracting electrons. This is due to the self-consistent-field nature of the Kohn-Sham equation (A2). In a more general formulation (i.e., beyond a Hartree-type response theory) the inclusion of exchange and correlation effects results in more complicated diagrams for the irreducible response.<sup>1,30</sup>

We note that Eq. (2.5) has the same form as the RPA integral equation for  $\chi$ .<sup>9,22</sup> In the RPA, however,  $V(\mathbf{x}_1, \mathbf{x}_2)$  is just the Coulomb potential [the first term on

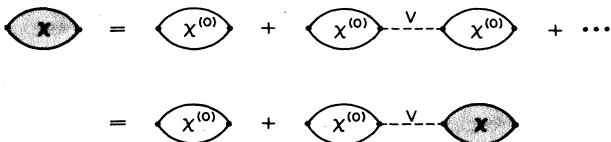


FIG. 1. Diagrammatic interpretation of the LDF integral equation for the density response function  $\chi(\mathbf{x}, \mathbf{x}')$  [Eq. (2.5)]. The electron-hole bubble  $\chi^{(0)}(\mathbf{x}, \mathbf{x}')$  is given by Eq. (A1), and the full electron-electron interaction  $V(\mathbf{x}_1, \mathbf{x}_2)$  is given by Eq. (2.6).

the right hand side of Eq. (2.6)]. A comparison of both approximations for  $\chi$  in the case of surface screening will be presented in Sec. III.

### B. Solution of the integral equation for a jellium slab

As indicated in the Introduction, in this paper we use the jellium model for the ionic background. This allows us to introduce the reduced density response function  $\chi(q_{\parallel} | z, z')$  defined by the equation

$$\chi(\mathbf{x}, \mathbf{x}') = \int \frac{d^2q_{\parallel}}{(2\pi)^2} e^{iq_{\parallel}(\mathbf{x}_{\parallel} - \mathbf{x}'_{\parallel})} \chi(q_{\parallel} | z, z'), \quad (2.7)$$

where  $q_{\parallel}$  is a two-dimensional wave vector in the plane of the surface [the plane  $(\mathbf{x}, \mathbf{y})$ ], and  $z$  denotes the coordinate normal to the surface. Note that in the jellium model the ground state is isotropic in the plane  $(\mathbf{x}, \mathbf{y})$  [in particular,  $n_0(\mathbf{x}) = n_0(z)$ ]; thus  $\chi(q_{\parallel} | z, z')$  depends on  $q_{\parallel}$  through its magnitude  $q_{\parallel}$  only.

Taking the two-dimensional Fourier transform of Eq. (2.5), according to Eq. (2.7), we are led to an integral equation for  $\chi(q_{\parallel} | z, z')$ , namely

$$\begin{aligned} \chi(q_{\parallel} | z, z') &= \chi^{(0)}(q_{\parallel} | z, z') \\ &+ \int dz_1 \int dz_2 \chi^{(0)}(q_{\parallel} | z, z_1) \\ &\quad \times V(q_{\parallel} | z_1, z_2) \chi(q_{\parallel} | z_2, z'), \end{aligned} \quad (2.8)$$

where the integrals run over the metal interior, and

$$V(q_{\parallel} | z_1, z_2) = \frac{2\pi e^2}{q_{\parallel}} e^{-q_{\parallel} |z_1 - z_2|} + \frac{dV_{\text{xc}}(z)}{dn_0(z)} \delta(z_1 - z_2). \quad (2.9)$$

The reduced response function for noninteracting electrons,  $\chi^{(0)}(q_{\parallel} | z, z')$ , is obtained in the Appendix. We have

$$\chi^{(0)}(q_{\parallel} | z, z') = \sum_{l=1}^{l_M} \sum_{l'=1}^{l'_M} F_{ll'}(q_{\parallel}) \phi_l(z) \phi_{l'}(z) \phi_l(z') \phi_{l'}(z'), \quad (2.10)$$

where the wave functions  $\phi_l(z)$  are the self-consistent solutions of the one-dimensional Kohn-Sham equation (A7), and the static electron-hole kernel  $F_{ll'}(q_{\parallel})$  is given explicitly by Eqs. (A16). The first sum in Eq. (2.10) runs over occupied energy levels only, the highest occupied level being denoted by  $l_M$ . The second sum in Eq. (2.10) runs over both occupied and unoccupied levels. Thus  $l'_M > l_M$ ; in principle,  $l'_M = \infty$ , cf. Eq. (A8). In the numerical calculations the value of  $l'_M$  must be large enough that the physical results are insensitive to the value chosen for it.

The result for  $\chi^{(0)}(q_{\parallel} | z, z')$  given by Eq. (2.10) is especially suited for the case of a jellium slab of finite width, in which case the spectrum of occupied one-dimensional levels for motion along the  $z$  axis is discrete. For example, for a jellium slab with the bulk density of aluminum and a thickness equal to fifteen atomic layers in the [100]

direction one has  $I_M = 17$ . Now, while the levels lying between the Fermi level and the vacuum level are also discrete, the states above the vacuum level form a continuum. However, the method of solution of Eq. (2.8) to be described below effectively replaces this continuum of states by a discrete set.

Equation (2.8) is solved as follows. We note that outside the jellium the electron density profile  $n_0(z)$  decays by several orders of magnitude within a distance of the order of  $2\pi/k_F$  from the jellium edge ( $k_F = 1.75 \text{ \AA}^{-1}$  for aluminum). It is then convenient to render the electronic system strictly finite in the  $z$  direction by assuming that  $n_0(z)$  actually vanishes at a finite distance (denoted by  $z_0$ ) from each edge of the jellium. (In reality the tail of the electron density profile is exponential.) We can then introduce the following double-cosine Fourier-series representation for the response function:<sup>7-11,22,31</sup>

$$\chi(q_{\parallel} | z, z') = \sum_{m=0}^{\infty} \sum_{n=0}^{\infty} \chi_{mn}(q_{\parallel}) \cos \left[ \frac{m\pi}{d} z \right] \cos \left[ \frac{n\pi}{d} z' \right], \quad (2.11)$$

which has the inverse transformation

$$\chi_{mn}(q_{\parallel}) = \frac{\mu_m \mu_n}{d^2} \int_0^d dz \int_0^d dz' \chi(q_{\parallel} | z, z') \times \cos \left[ \frac{m\pi}{d} z \right] \cos \left[ \frac{n\pi}{d} z' \right], \quad (2.12)$$

$$V_{mn}^{(c)}(q_{\parallel}) = \frac{2\pi e^2}{q_{\parallel}^2 + (m\pi/d)^2} \left[ \frac{2d}{(\mu_m \mu_n)^{1/2}} \delta_{mn} - [1 + (-1)^{m+n}] \frac{q_{\parallel} [1 - (-1)^m e^{-q_{\parallel} d}]}{q_{\parallel}^2 + (n\pi/d)^2} \right], \quad (2.17)$$

and the matrix elements  $V_{mn}^{(xc)}$  of the exchange and correlation interaction are defined by the equation

$$V_{mn}^{(xc)} = \int_0^d dz \frac{dV_{xc}(z)}{dn_0(z)} \cos \left[ \frac{m\pi}{d} z \right] \cos \left[ \frac{n\pi}{d} z \right]. \quad (2.18)$$

From Eqs. (2.10) and (2.12) we have that the matrix of the coefficients  $\chi_{mn}^{(0)}(q_{\parallel})$  of the noninteracting electron response is given by the equation

$$\chi_{mn}^{(0)}(q_{\parallel}) = \frac{\mu_m \mu_n}{d^2} \sum_{l=1}^{I_M} \sum_{l'=1}^{I'_M} F_{ll'}(q_{\parallel}) G_{ll'}^m G_{ll'}^n, \quad (2.19)$$

where

$$G_{ll'}^m \equiv \int_0^d dz \cos \left[ \frac{m\pi}{d} z \right] \phi_l(z) \phi_{l'}(z). \quad (2.20)$$

We solve Eq. (2.15) numerically using standard routines. We have not encountered the numerical problems that led Rasolt and Perrot<sup>1</sup> and Maniv and Metiu<sup>31</sup> to carry out rather lengthy reformulations of response equations of the form of Eq. (2.15) before solving them numerically (in the case of Ref. 1, this was done by iteration).

where the coefficients  $\mu_m$  (the Neumann numbers) are defined by the equation

$$\mu_m = \begin{cases} 1 & \text{for } m=0, \\ 2 & \text{for } m \geq 1. \end{cases} \quad (2.13)$$

The length  $d$  introduced in Eq. (2.11) is given by the equation

$$d = a + 2z_0, \quad (2.14)$$

$a$  being the width of the jellium slab. Thus  $d$  is the width of the electronic system in the  $z$  direction. Note that in Eq. (2.11) we have set the origin of coordinates on the left-hand edge of the film.

Substituting Eq. (2.11) and a similarly defined representation for  $\chi^{(0)}(q_{\parallel} | z, z')$  into Eq. (2.8), we obtain the following matrix equation for the coefficients  $\chi_{mn}(q_{\parallel})$  of the response:

$$\chi_{mn}(q_{\parallel}) = \chi_{mn}^{(0)}(q_{\parallel}) + \sum_{m', n'} \chi_{mm'}^{(0)}(q_{\parallel}) V_{m'n'}(q_{\parallel}) \chi_{n'n}(q_{\parallel}), \quad (2.15)$$

where we have made the definition

$$V_{mn}(q_{\parallel}) \equiv V_{mn}^{(c)}(q_{\parallel}) + V_{mn}^{(xc)}, \quad (2.16)$$

where the matrix elements  $V_{mn}^{(c)}(q_{\parallel})$  of the Coulomb interaction are given explicitly by the equation

### C. Numerical procedure

In this section we comment on the procedure that we have used in the computation of the ingredients of Eq. (2.15), namely the matrices  $\chi_{mn}^{(0)}(q_{\parallel})$  and  $V_{mn}(q_{\parallel})$ .

The assumption made in the derivation of Eq. (2.15) that  $n_0(z)$  vanishes at a distance  $z_0$  from the jellium edge implies, from the point of view of the differential equation (A7), the introduction of infinite potential walls at a distance  $z_0$  from each edge of the jellium. We then introduce the following representation for the wave functions  $\phi_l(z)$ :

$$\phi_l(z) = \left[ \frac{2}{d} \right]^{1/2} \sum_{s=1}^{\infty} b_{ls} \sin \left[ \frac{s\pi}{d} z \right], \quad (2.21)$$

which automatically satisfies the boundary conditions that  $\phi_l(z) = 0$  at  $z = 0$  and  $z = d$ .

A procedure has recently been given for computing the coefficients  $b_{ls}$  self-consistently.<sup>17</sup> It consists in transforming Eq. (A7) into a matrix equation through the use of Eq. (2.21). Since  $V_{\text{eff}}(z)$  is a functional of  $n_0(z)$ , which itself is a quadratic function of the  $\{b_{ls}\}$ , one is led to a nonlinear self-consistent matrix eigenvalue problem. Its solution is discussed in Ref. 17.

With the representation (2.21) for the wave functions  $\phi_l(z)$  the integral required in Eq. (2.20) is elementary. We have

$$G_{ll'}^m = \frac{1}{2} \sum_{s=1}^{\infty} \sum_{s'=1}^{\infty} b_{ls} b_{l's'} (\delta_{m,s-s'} + \delta_{m,s'-s} - \delta_{m,s+s'}) . \quad (2.22)$$

Equation (2.22) together with Eqs. (A16) and Eq. (2.19) give an explicit result for the Fourier coefficients  $\chi_{mn}^{(0)}(q_{\parallel})$  of the response function for noninteracting electrons. We emphasize that this result is in a form particularly suited for its numerical computation since it only involves matrix algebra [to be carried out on the basis of the knowledge of the coefficients  $b_{ls}$  defined by Eq. (2.21)].

Of course, in practice one approximates Eq. (2.21) by a finite series. Let us call  $s_{\max}$  the number of terms (sines) in that series. From Eq. (2.22) it immediately follows that  $G_{ll'}^m = 0$  for  $m > 2s_{\max}$ . Thus the rank of the matrix  $\chi_{mn}^{(0)}(q_{\parallel})$  [and that of the matrix  $\chi_{mn}(q_{\parallel})$ ] equals  $2s_{\max} + 1$ .

Now the density profile  $n_0(z)$  is symmetric about the midplane of the slab, and thus so are any other properties of the ground state. In the case of the response function  $\chi^{(0)}(q_{\parallel} | z, z')$  the reflection symmetry about the midplane is stated as

$$\chi^{(0)}(q_{\parallel} | d - z, d - z') = \chi^{(0)}(q_{\parallel} | z, z') . \quad (2.23)$$

From Eqs. (2.12) and (2.23) we have that  $\chi_{mn}^{(0)}(q_{\parallel}) = 0$  if  $m$  and  $n$  are of opposite parity ( $m$  even and  $n$  odd, or vice versa). In fact all the matrices that enter Eq. (2.15) share this property. Thus, Eq. (2.15) decouples into two sets of equations for the even and odd parts of  $\chi_{mn}(q_{\parallel})$ , respectively. This is very convenient from a numerical standpoint, since then we only have to work with matrices whose rank is half that of the full matrix  $\chi_{mn}(q_{\parallel})$ .

The above formulation introduced three numerical parameters whose values must be sufficiently large that the physical results are independent of them. They are the distance  $z_0$ , the number of sines  $s_{\max}$  kept in Eq. (2.21), and the upper limit  $l'_M$  in Eqs. (2.19). Examples are given in Sec. III. A type of problem that demands high accuracy in the computation of the electron response is one involving the subtraction of two quantities of nearly equal magnitude. An example of this situation is encountered in Sec. III. Dynamical response problems are also numerically demanding whenever levels lying substantially above the vacuum level contribute to the response.<sup>22</sup> Those levels depend sensitively on  $z_0$ , that is, on the position of the fictitious infinite barriers relative to the jellium edges.

We would like to emphasize that for the values of  $z_0$  and  $s_{\max}$  for which the response function is known with sufficient accuracy the electron density profile obtained from Eq. (2.21) agrees extremely well with the Lang-Kohn profile<sup>15</sup> throughout the surface region about each jellium edge.<sup>17</sup>

A technical difficulty in the evaluation of the matrix  $V_{mn}^{(xc)}$  [defined by Eq. (2.18)] must be noted. Using the local Slater approximation for exchange reduced by a factor of  $\frac{2}{3}$ , and the local Wigner interpolation for correlation,<sup>18</sup> we have that the density derivative of  $V_{xc}(z)$  required in

Eq. (2.18) is given by the equation

$$\frac{dV_{xc}(z)}{dn_0(z)} = -\frac{2}{9} e^2 n_0^{-2/3}(z) F_{xc}(z) , \quad (2.24)$$

where

$$F_{xc}(z) \equiv \frac{3}{2} \left[ \frac{3}{\pi} \right]^{1/3} + 0.056 \times 0.079 \frac{0.158 + a_B n_0^{1/3}(z)}{[0.079 + a_B n_0^{1/3}(z)]^3} , \quad (2.25)$$

$a_B$  being the Bohr radius. Now, the electron density profile  $n_0(z)$  has been assumed to vanish at  $z=0$  and  $z=d$ . With the representation of the wave functions  $\phi_l(z)$  given by Eq. (2.21) we have that  $n_0(z) \sim z^2$  as  $z \rightarrow 0$ . (Because of reflection symmetry the present argument need only be made for  $z=0$ .) Thus  $dV_{xc}(z)/dn_0(z)$  behaves like  $z^{-4/3}$  as  $z \rightarrow 0$  and Eq. (2.18) has an end-point singularity. It is easy to see that the root of this problem is the cosine representation for the response function introduced in Eq. (2.11). In effect, from Eqs. (2.10) and (2.21) we have that  $\chi^{(0)}(q_{\parallel} | z, z_1) \sim z_1^2$  as  $z_1 \rightarrow 0$ . From the structure of Eq. (2.8) it follows that also  $\chi(q_{\parallel} | z_1, z') \sim z_1^2$  as  $z_1 \rightarrow 0$ . Thus, the contribution to the integrand in Eq. (2.8) from the exchange-correlation potential behaves like  $z_1^{8/3}$  as  $z_1 \rightarrow 0$ . The integral equation for  $\chi(q_{\parallel} | z, z')$  is then well defined. Had we used a sine representation instead of Eq. (2.11), the present problem with Eq. (2.18) would not arise. Since we do use Eq. (2.11) [basically because it leads to the simple result given by Eq. (2.22), which fixes the rank of the matrix  $\chi_{mn}$  to be  $2s_{\max} + 1$ ], we proceed as follows. We introduce a finite lower limit in the integral (2.18) and carry out the computations keeping this lower limit as a parameter. Since, as noted above, the original integral equation (2.8) is well behaved, we are sure to obtain convergent results for sufficiently small values of this parameter.

We close this section with a comment on the philosophy of the above formulation. It is obvious that our method is suitable for the study of intrinsic thin-film effects. However, our main interest is in the study of the response of a semi-infinite medium. That our method does give a good representation of the static response of a semi-infinite medium<sup>32</sup> (while involving matrices of moderate rank) is because of two basic reasons. First we have that the static electron screening length  $2\pi/k_F$  is, at metallic densities, of the order of a few angstroms. This is why for films thicker than 5–10 atomic layers (the “threshold” thickness depends on the bulk electron density, i.e., on  $k_F$ ) the electron density profile is, in the surface region about each jellium edge, the same as that for a semi-infinite slab.<sup>17</sup> In this sense, in the ground state the two slab surfaces are decoupled. Second, in screening processes involving a surface impurity typical two-dimensional wave-vector transfers are large [of  $O(k_F)$ ]. Thus, for fairly thin films (films not much thicker than about 10 atomic layers) we have that  $q_{\parallel} d \gg 1$ , and the external source effectively “sees” only one of the slab surfaces.

### III. ELECTRON DENSITY INDUCED BY AN IMPURITY PLACED NEAR THE SURFACE

As noted in the Introduction, a basic feature of metallic behavior is the screening response of the conduction electrons to a local charge imbalance. This can arise because of the presence of an embedded impurity, of an adsorbed atom or molecule, or of the ion cores of the metal itself. The latter case brings the screening process into the context of the lattice dynamics of metal surfaces. The screening of the ions by the electrons gives rise to an indirect interaction between the ions which added to their bare interaction gives the total ion-ion interaction, from which quantities such as lattice relaxation and surface-phonon dispersion relations can be obtained.<sup>5,6</sup> This application of the response function obtained in Sec. II is in progress and it will be reported elsewhere.<sup>24</sup> Here we will consider what is, in essence, the "building block" of the surface screening process, namely the electron density induced by an impurity placed near the surface. This is given by Eq. (2.1), with

$$U_{\text{ext}}(\mathbf{x}) = -\frac{eQ}{|\mathbf{x} - \mathbf{x}_1|}, \quad (3.1)$$

where  $Q$  denotes the charge of the impurity and  $\mathbf{x}_1$  its position vector. Without loss of generality in what follows we set  $\mathbf{x}_1 = (0, 0, z_1)$ , i.e., we place the impurity on the  $z$  axis. Unless otherwise specified we measure the coordinate  $z$  from the left edge of the film.

$$A_n(q_{\parallel} | z_1) = \begin{cases} -[(-1)^n e^{-q_{\parallel} d} - 1] e^{q_{\parallel} z_1}, & z_1 \leq 0 \\ 2 \cos \left[ \frac{n\pi}{d} z_1 \right] - [e^{-q_{\parallel} z_1} + (-1)^n e^{-q_{\parallel} (d - z_1)}], & 0 \leq z_1 \leq d \\ [(-1)^n - e^{-q_{\parallel} d}] e^{-q_{\parallel} (z_1 - d)}, & z_1 \geq d. \end{cases} \quad (3.5a)$$

$$A_n(q_{\parallel} | z_1) = \begin{cases} -[(-1)^n e^{-q_{\parallel} d} - 1] e^{q_{\parallel} z_1}, & z_1 \leq 0 \\ 2 \cos \left[ \frac{n\pi}{d} z_1 \right] - [e^{-q_{\parallel} z_1} + (-1)^n e^{-q_{\parallel} (d - z_1)}], & 0 \leq z_1 \leq d \\ [(-1)^n - e^{-q_{\parallel} d}] e^{-q_{\parallel} (z_1 - d)}, & z_1 \geq d. \end{cases} \quad (3.5b)$$

$$A_n(q_{\parallel} | z_1) = \begin{cases} -[(-1)^n e^{-q_{\parallel} d} - 1] e^{q_{\parallel} z_1}, & z_1 \leq 0 \\ 2 \cos \left[ \frac{n\pi}{d} z_1 \right] - [e^{-q_{\parallel} z_1} + (-1)^n e^{-q_{\parallel} (d - z_1)}], & 0 \leq z_1 \leq d \\ [(-1)^n - e^{-q_{\parallel} d}] e^{-q_{\parallel} (z_1 - d)}, & z_1 \geq d. \end{cases} \quad (3.5c)$$

Equations (3.5a) and (3.5c) correspond to the case in which the impurity is outside the electron system (to the left or to the right of the film, respectively), and Eq. (3.5b) corresponds to the case in which the impurity is inside it.

Now, since charge is conserved in the screening process, the integral of Eq. (3.2) over the volume occupied by the film must equal  $Q/e$ . This condition translates into the (exact) result that

$$\int_0^d dz n_{\text{ind}}(q_{\parallel} = 0 | z) = \frac{Q}{e}. \quad (3.6)$$

Substituting either Eq. (3.5a) or Eq. (3.5c) into Eq. (3.4), Eq. (3.6) leads us to the result that

$$\lim_{q_{\parallel} \rightarrow 0} \left[ \frac{\chi_{00}(q_{\parallel})}{q_{\parallel}} \right] = -\frac{1}{2\pi e^2 d^2}. \quad (3.7)$$

Performing the same calculation but using Eq. (3.5b) we obtain, in addition to Eq. (3.7), the condition that, for  $n > 0$ ,

$$\lim_{q_{\parallel} \rightarrow 0} \chi_{0n}(q_{\parallel}) = 0. \quad (3.8)$$

Equations (3.7) and (3.8) are direct consequences of

The usual relation between  $n_{\text{ind}}(\mathbf{x})$  and its two-dimensional Fourier transform  $n_{\text{ind}}(q_{\parallel} | z)$  [cf. Eq. (2.7)] can be rewritten as

$$n_{\text{ind}}(\mathbf{x}) = \frac{1}{2\pi} \int_0^{\infty} dq_{\parallel} q_{\parallel} J_0(q_{\parallel} R_{\parallel}) n_{\text{ind}}(q_{\parallel} | z), \quad (3.2)$$

where  $J_0(x)$  is the Bessel function of order 0, and  $R_{\parallel} \equiv |\mathbf{x}_{\parallel}|$ . Taking the Fourier transform of Eq. (2.1) according to Eq. (2.7) we have that

$$n_{\text{ind}}(q_{\parallel} | z) = -\frac{2\pi e Q}{q_{\parallel}} \int_0^d dz' e^{-q_{\parallel} |z' - z|} \chi(q_{\parallel} | z, z'), \quad (3.3)$$

where the argument of the exponential brings in the dependence of  $n_{\text{ind}}(q_{\parallel} | z)$  on the position of the impurity. This dependence has been omitted in the above notation.

Substituting Eq. (2.11) in Eq. (3.3) we obtain, for  $0 \leq z \leq d$ ,

$$n_{\text{ind}}(q_{\parallel} | z) = -2\pi e Q \sum_{m,n} \chi_{mn}(q_{\parallel}) \cos \left[ \frac{m\pi}{d} z \right] \times \frac{A_n(q_{\parallel} | z_1)}{q_{\parallel}^2 + (n\pi/d)^2}. \quad (3.4)$$

For  $z \geq d$  or  $z \leq 0$  (i.e., outside the electron system)  $n_{\text{ind}}(q_{\parallel} | z) = 0$ . The function  $A_n(q_{\parallel} | z_1)$  introduced in Eq. (3.4) is defined as follows:

charge conservation. They are satisfied by our numerical results. Equation (3.7), in particular, is typically verified to six significant figures.

It is interesting to note (and not difficult to prove) that the charge-conservation condition given by Eq. (3.7) ensures that the static image potential experienced by an electron has the asymptotic form  $-e^2/4z$  (independent of the film thickness).

In Figs. 2–5 we present numerical results for the induced density (we have set  $Q = e$ ) for the case of a jellium slab with the bulk density of aluminum and a thickness equal to 11 atomic layers of Al in the [100] direction ( $a = 22.2 \text{ \AA}$ ). It was verified that our results do not change, on the scale of the figure, if thicker films are used. Thus the results of Figs. 2–5 can be thought of as pertaining to a semi-infinite medium. The physical reasons behind this conclusion were given at the end of Sec. II.

In Fig. 2 we show  $n_{\text{ind}}(\mathbf{x})$  for points in the plane parallel to the surface that contains the impurity (i.e., for  $z = z_1$ ), as a function of the lateral distance  $R_{\parallel}$  from the impurity, for several values of the position  $z_1$  of the impurity relative to the right-hand edge of the jellium ( $z_1$  is

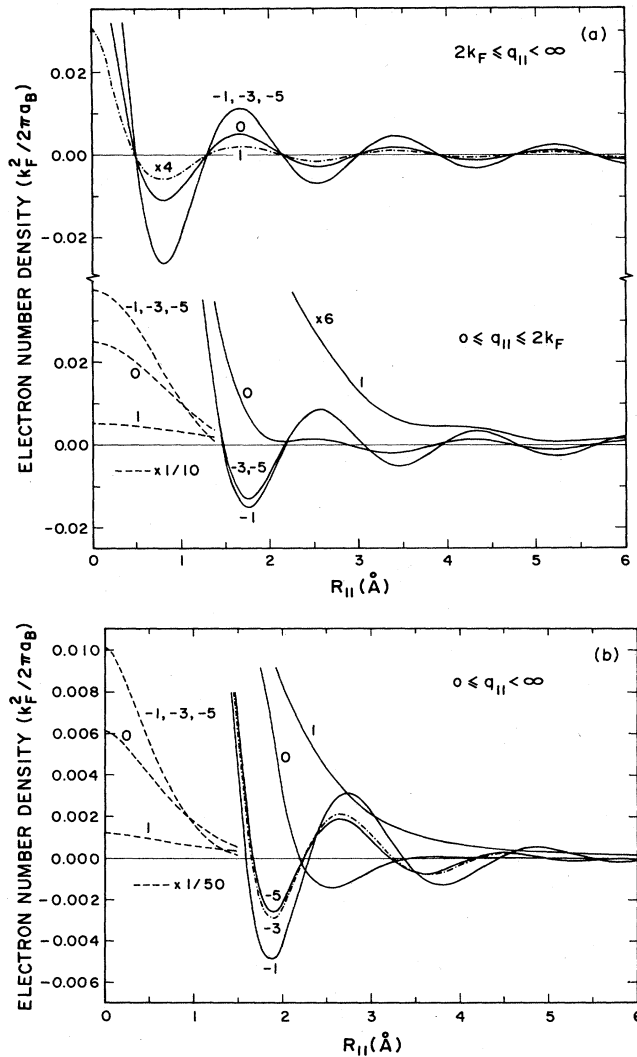


FIG. 2. Electron number density induced by an impurity of charge  $Q=e$  at points in the plane parallel to the surface that contains the impurity. The jellium has the bulk density of aluminum. The induced density is given in units of  $k_F^2/2\pi a_B$ , where  $a_B$  is the Bohr radius. The curves are labeled by the distance  $z_1$  (in Å) between the impurity and the right edge of the jellium ( $z < 0$  means inside the jellium). (a) Separate contributions to Eq. (3.2) from  $0 \leq q_{||} \leq 2k_F$  and  $2k_F \leq q_{||} \leq \infty$ , respectively. (b) Total induced density  $n_{ind}(x)$ .

measured in Å). The analysis of Figs. 2(a) and 2(b) is best done by recalling that Lau and Kohn<sup>4</sup> have (in effect) proved that  $\chi^{(0)}(q_{||}|z, z')$  has weak singularities at  $q_{||} = 2k_F$ . The leading singularity is of the form  $(q_{||} - 2k_F)^{7/2}$  for  $q_{||} \rightarrow 2k_F$  from above. The structure of Eq. (2.8) [and of Eq. (2.15)] suggests that this singular behavior at  $2k_F$  is shared by the full-response function  $\chi(q_{||}|z, z')$ . This is corroborated by the results shown in Fig. 2(a), which displays the separate contributions to Eq. (3.2) from the intervals  $0 \leq q_{||} \leq 2k_F$  and  $2k_F \leq q_{||} \leq \infty$ . Each contribution to  $n_{ind}(x)$  shows long-range oscillations of period  $\pi/k_F$ . This, according to the asymptotic

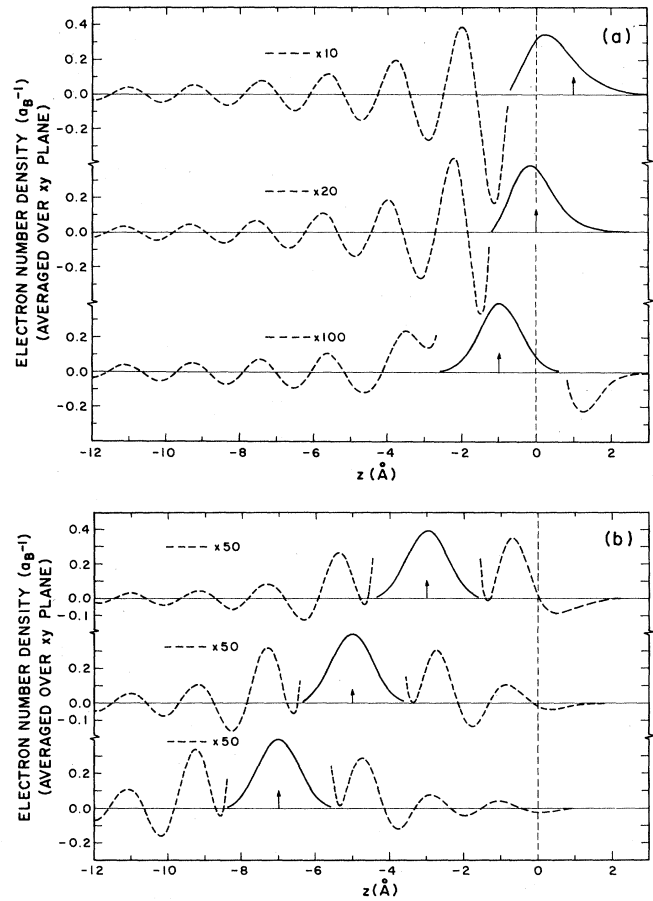


FIG. 3. Electron number density (averaged over the  $x$ - $y$  plane) induced by an impurity of charge  $Q=e$  at points on the axis normal to the surface. The jellium has the bulk density of aluminum. The induced density is given in units of the Bohr radius. The long-range oscillations have been magnified by the factor shown in each panel. (b)  $\bar{n}_{ind}(z)$  for  $z_1 = -7, -5$ , and  $-3$  Å. (a)  $\bar{n}_{ind}(z)$  for  $z_1 = -1$  Å, 0, and 1 Å. All distances are measured from the right edge of the jellium.

analysis of integrals of the form of Eq. (3.2),<sup>33</sup> reveals the existence of a singularity in the integrand (that is, in  $\chi$ ) for  $q_{||} \rightarrow 2k_F$ .

Now, the analysis of Ref. 4 would predict that the amplitude of the oscillations in the upper panel of Fig. 2(a) would decay as  $R_{||}^{-5}$ . For the values of  $R_{||}$  considered in the figure, the decay rate is much slower (somewhat faster than linear). Thus the fifth power decay rate must take hold farther away from the impurity than typical nearest-neighbor distances in metals. We note that the decay rate of the oscillations in the total induced density shown in Fig. 2(b) (roughly  $\sim R_{||}^{-3}$ ) is faster than the decay rate for either of the two contributions to it [Fig. 2(a)]. We remark that for the values of  $R_{||}$  considered here our numerical results cannot be fitted by a simple inverse-power decay law. These conclusions agree with the analytical IBM results of Johansson<sup>3</sup> and Johansson and Hjelmberg,<sup>3</sup> who studied the possible connection between the oscillations in  $n_{ind}(x)$  and low-energy electron

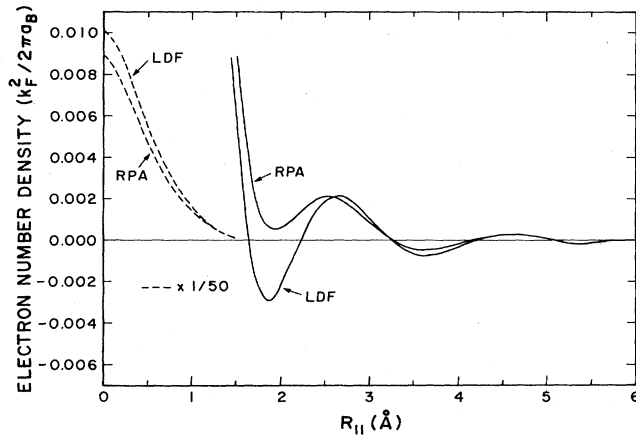


FIG. 4. Induced density  $n_{\text{ind}}(\mathbf{x})$  in the LDF and RPA approximations (see text). The impurity has been placed at  $z_1 = -2 \text{ \AA}$ , inside the jellium [cf. Fig. 2(b)].

diffraction (LEED) patterns. It is important to note the rapid decrease of the amplitude of the oscillations in Fig. 2(a) as the impurity is moved outward through the surface region. We also note that the oscillations in the lower panel are out of phase by nearly half a wavelength relative to those in the upper panel. The latter result gives rise to a substantial cancellation in the addition of both contributions to  $n_{\text{ind}}(\mathbf{x})$ . [Note the change in the vertical scale in Fig. 2(b).]

The main feature of the result for the total induced density  $n_{\text{ind}}(\mathbf{x})$  shown in Fig. 2(b) is the disappearance of the long-range oscillatory behavior when the impurity is placed outside the jellium ( $z_1 > 0$ ). The monotonic decay of the curve for  $z_1 = 1 \text{ \AA}$  is determined by the behavior of the integrand of Eq. (3.2) for  $q_{\parallel} \rightarrow 0$ . We also note that the effect of the surface on the magnitude of the charge buildup near the impurity [shown in dashes in Fig. 2(b)] is short ranged: It is the same (on the scale of the figure) for

$z_1$  deeper than one angstrom into the metal. On the other hand, the effect of the surface on the long-range lateral oscillations is felt rather deeper into the metal. The implications of the above results for the lateral interaction between two charges placed in the surface region have been given recently.<sup>17</sup>

In Fig. 3 we show results for the density induced along the  $z$  axis for six different positions of the impurity, ranging from "deep inside" the jellium ( $z_1 = -7 \text{ \AA}$ ) to  $z_1 = 1 \text{ \AA}$  outside it. (In each case the location of the impurity is denoted by an arrow.) For the sake of simplicity we only consider the induced density averaged over the  $x$ - $y$  plane,  $\bar{n}_{\text{ind}}(z)$ , given by the equation

$$\bar{n}_{\text{ind}}(z) \equiv \int d^2x_{\parallel} n_{\text{ind}}(\mathbf{x}) = n_{\text{ind}}(q_{\parallel} = 0 | z). \quad (3.9)$$

According to Eq. (3.6) the area under all the curves in Fig. 3 must be the same. This is verified by our results to high accuracy.

We would like to comment upon two features of the results shown in Fig. 3. First we note that, as found before by other authors,<sup>25,34</sup> the density buildup near the impurity becomes asymmetric, and the centroid of the induced density lags behind the impurity, as this is moved outwards through the jellium edge. We find that the centroid of the induced charge is already within 1% of its asymptotic value (corresponding to  $z_1 \rightarrow \infty$ ) for  $z_1 \sim 3 \text{ \AA}$ . Second, we note the left-right asymmetry in the long-range oscillations in  $\bar{n}_{\text{ind}}(z)$ . We remark that their amplitude is largest when the impurity is at the jellium edge or outside it. (Note the change in the scales used in the various panels in Fig. 3.) Now the lateral oscillations shown in Fig. 2 had their origin in the singularity of the response function for  $q_{\parallel} = 2k_F$ . In the present case we have set  $q_{\parallel} = 0$ . Since the long-range oscillations shown in Fig. 3(a) [and also in Fig. 3(b) for values of  $z$  to the left of the impurity] have period  $\pi/k_F$ , they must have their origin in a singularity of the response function for  $q_z = 2k_F$ , where  $q_z (\cong n\pi/d)$  is an effective wave vector normal to

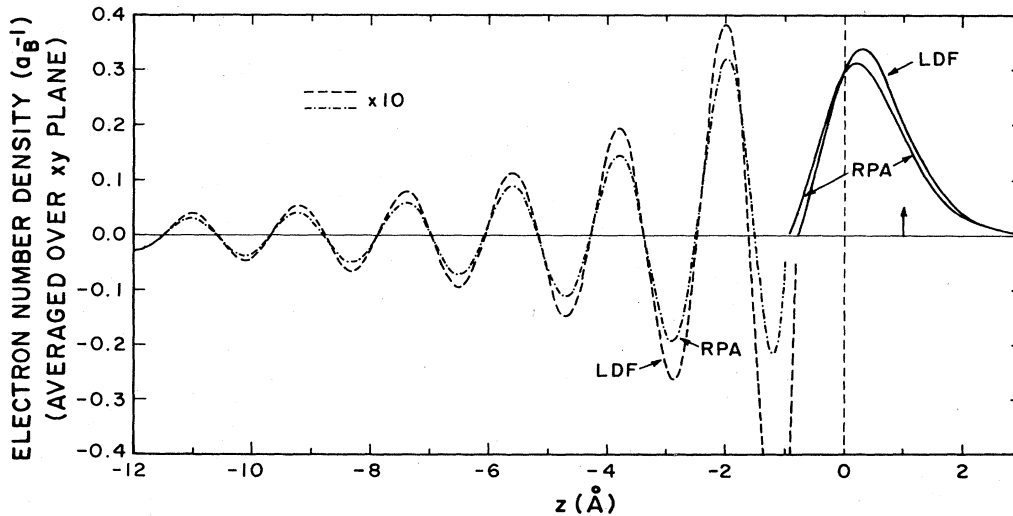


FIG. 5. Induced density  $\bar{n}_{\text{ind}}(z)$  averaged over the  $x$ - $y$  plane in the LDF and RPA approximations (see text). The impurity has been placed at  $z_1 = 1 \text{ \AA}$  outside the jellium [cf. Fig. 3(b)].

the surface. It is very satisfying that we are able to bring up this feature of the long-range screening density with our thin-film calculation, in which we carry out a sum (not an integral) over the discrete sequence of wave vectors  $n\pi/d$  [cf. Eq. (3.4)].

We recall that the solution for the response function given in Sec. II includes three numerical parameters ( $z_0$ ,  $s_{\max}$ , and  $l'_M$ ) which must be adjusted in such a way that the computed observables are independent of the values chosen for them. The results of Figs. 2–5 have converged, on the scale of each figure, for  $z_0 = 1.5a_0$  (where  $a_0$  is the lattice constant:  $a_0 = 4.05 \text{ \AA}$  for aluminum),  $s_{\max} \cong 80$  and  $l'_M \cong 80$ . The most demanding part of the computation is the long-range oscillatory regime. In the case of the lateral oscillations shown in Fig. 2, there are two complicating features: the above-mentioned cancellation that obtains on adding the two panels of Fig. 2(a), and the fact that the integrand in Eq. (3.2) decays rather slowly for large values of  $q_{\parallel}$  (the upper limit of the integral has to be  $\geq 11k_F$  for convergence). For large  $q_{\parallel}$  ( $q_{\parallel} \gg k_F$ ) electron “subbands” with  $l' > l_M$  give a relatively larger contribution to Eq. (2.19) than they do for small  $q_{\parallel}$ . If we require convergence of the long-range lateral oscillations to 1–5% everywhere, larger values of  $l'_M$  than given above are required ( $l'_M > 100$ ).

Finally, in Figs. 4 and 5 we illustrate the effect exchange and correlation have on the screening density (and thus indirectly on  $\chi$ ) by comparing results obtained in the LDF and RPA approximations. To be precise, what we compare is the effect of using in Eq. (2.8) either the full electron-electron interaction given by Eq. (2.9) (LDF) or just the Coulomb interaction (RPA). In both cases we use the same single-particle wave functions  $\phi_l(z)$  in the computation of  $\chi^{(0)}$  [the solutions to Eq. (A7) with  $V_{\text{eff}}(z)$  given by the Lang-Kohn surface potential]. Figure 4 corresponds to Fig. 2(b) for the case that  $z_1 = -2 \text{ \AA}$ . Figure 5 corresponds to Fig. 3(a) for the case that  $z_1 = 1 \text{ \AA}$ . The qualitative agreement between the results obtained in both approximations is apparent. There are, however, quantitative differences. For example, the position of the centroid of the induced charge (which we denote by  $z_c$ , and measure from the jellium edge) in Fig. 5 differs markedly in both approximations:  $z_c = 0.61 \text{ \AA}$  in LDF and  $z_c = 0.45 \text{ \AA}$  in RPA. For the case that  $z_1 = \infty$  we find that  $z_c = 0.84 \text{ \AA}$  in LDF and  $z_c = 0.65 \text{ \AA}$  in RPA. (Our LDF result is in excellent agreement with the result obtained by Lang and Kohn<sup>15</sup> for semi-infinite jellium with  $r_s = 2$ .) Note that in the latter case  $z_c$  coincides with the position of the effective image plane,<sup>15,34</sup> a quantity of importance in physisorption studies<sup>35</sup> and in the analysis of large-angle, high-resolution electron-energy-loss spectroscopy (EELS).<sup>36</sup>

The above result illustrates the sensitivity of surface screening to the physical model used in the evaluation of the response function. Clearly, for quantitative purposes a self-consistent response calculation (such as the one reported here) is required.

#### IV. CONCLUDING REMARKS

We have obtained the static density response function of a jellium slab in the LDF approximation. Our formu-

lation is straightforward to implement. The calculation of physical observables is reduced to carrying out matrix algebra on the computer on the basis of the knowledge of the matrix  $\chi_{mn}(q_{\parallel})$  (which itself is obtained by matrix methods). The overall accuracy of a given computation is controllable, and any residual thin-film effects can be estimated. The accuracy (and the computer time) increases as the values of the three numerical parameters introduced by our formulation ( $z_0$ ,  $s_{\max}$ , and  $l'_M$ ) are increased. An example of the use of the method was given in Sec. III. Our method is currently being applied in a first-principles computation of quantities that can be compared directly with experiment, such as lattice relaxation at a (simple) metal surface and surface-phonon dispersion relations.<sup>24</sup>

We would like to note that the present paper has been restricted to the study of the *static* electronic response by our use of density-functional theory in obtaining the exchange and correlation contribution to the kernel of Eq. (2.8) [and by our use of the wave functions  $\phi_l(z)$  of density-functional theory]. Recently several authors<sup>37–40</sup> have invoked an adiabatic ansatz that involves using static response functions in the study of low-frequency interactions near a surface, such as low-energy EELS<sup>37</sup> and damping of adsorbate vibrations.<sup>37–40</sup> In a similar spirit we plan to consider the use of Eq. (2.8) with  $\chi^{(0)}$  given by the full finite-frequency result obtained in the Appendix. Since our method of solution of Eq. (2.8) proceeds in the same way for  $\omega \neq 0$ , we would then have a quasistatic self-consistent density response function that could be of use in the study of low-frequency dynamical surface processes. In fact, very recently Liebsch has calculated the lifetime of a vibrational mode of an adsorbate using similar ideas.<sup>40</sup>

#### ACKNOWLEDGMENT

I am grateful to Professor A. A. Maradudin and Professor R. F. Wallis for their support. This work was supported by the National Science Foundation under Grant No. DMR-82-14214.

#### APPENDIX: NONINTERACTING ELECTRON RESPONSE FUNCTION FOR A METAL SLAB

Although the subject matter of the present paper is *static* surface screening, in this appendix it is convenient to begin by consider the *dynamical* response function for noninteracting electrons,  $\chi^{(0)}(\mathbf{x}, \mathbf{x}' | \omega)$ , defined at  $T = 0 \text{ K}$  by the equation<sup>9</sup>

$$\chi^{(0)}(\mathbf{x}, \mathbf{x}' | \omega) = \sum_{\nu, \nu'} \frac{f_{\nu} - f_{\nu'}}{E_{\nu} - E_{\nu'} - \hbar(\omega + i\eta)} \psi_{\nu}(\mathbf{x}) \psi_{\nu'}^*(\mathbf{x}) \psi_{\nu'}(\mathbf{x}') \psi_{\nu}^*(\mathbf{x}'), \quad (\text{A1})$$

with  $f_{\nu} = 2\Theta(E_F - E_{\nu})$ , where  $E_F$  is the Fermi energy,  $\Theta(x)$  is the unit step function,  $\omega$  is the frequency, and  $\eta$  is a positive infinitesimal. The static response function  $\chi^{(0)}(\mathbf{x}, \mathbf{x}')$  defined by Eq. (2.2) is given by the  $\omega = 0$  limit of Eq. (A1), i.e.,

$$\chi^{(0)}(\mathbf{x}, \mathbf{x}') \equiv \chi^{(0)}(x, x' | \omega = 0). \quad (\text{A2})$$

The single-particle wave functions  $\psi_v(\mathbf{x})$  and energy eigenvalues  $E_v$  are assumed to be the solutions of the Kohn-Sham equation<sup>18</sup>

$$\left[ -\frac{\hbar^2}{2m} \nabla^2 + V_{\text{eff}}(\mathbf{x}) \right] \psi_v(\mathbf{x}) = E_v \psi_v(\mathbf{x}), \quad (\text{A3})$$

where the effective potential  $V_{\text{eff}}(\mathbf{x})$  is given by

$$V_{\text{eff}}(\mathbf{x}) = v(\mathbf{x}) + e^2 \int d^3x' \frac{n(\mathbf{x}')}{|\mathbf{x} - \mathbf{x}'|} + V_{\text{xc}}(\mathbf{x}). \quad (\text{A4})$$

In Eq. (A4)  $v(\mathbf{x})$  is the potential for the interaction with the ionic background (in the present work modeled by a jellium), the second term is the electrostatic energy, and  $V_{\text{xc}}(\mathbf{x})$  denotes the exchange and correlation potential. In the present work the local-density approximation for  $V_{\text{xc}}(\mathbf{x})$  is adopted.<sup>18</sup> For the exchange potential we use the local Slater approximation reduced by a factor of  $\frac{2}{3}$ , and for the correlation potential we use the local Wigner interpolation.<sup>18</sup>

It is to be noted that only for  $\omega = 0$  is the use in Eq. (A1) of the solutions to the Kohn-Sham equation strictly legitimate. The static response function is, according to density-functional theory, a functional of the electron density  $n(\mathbf{x})$  and thus of the wave functions  $\psi_v(\mathbf{x})$  obtained solving Eqs. (A3) and (A4) self-consistently. A rigorous extension of density-functional theory to dynamical response remains an outstanding problem. (A phenomenological approach was given some time ago by Ying.<sup>41</sup>)

$$F_{ll'}(q_{\parallel}, \omega) = -\frac{1}{\hbar A} \sum_{\mathbf{k}_{\parallel}} f_{\mathbf{k}_{\parallel} l} \left[ \frac{1}{(\hbar/m) \mathbf{q}_{\parallel} \cdot \mathbf{k}_{\parallel} + a_{ll'}(q_{\parallel}) + \omega + i\eta} + \frac{1}{(\hbar/m) \mathbf{q}_{\parallel} \cdot \mathbf{k}_{\parallel} + a_{ll'}(q_{\parallel}) - \omega - i\eta} \right], \quad (\text{A9})$$

with

$$a_{ll'}(q_{\parallel}) = \frac{\hbar}{2m} q_{\parallel}^2 - \frac{1}{\hbar} (\epsilon_l - \epsilon_{l'}). \quad (\text{A10})$$

Three features of the representation of  $\chi^{(0)}(q_{\parallel}, \omega | z, z')$  given by Eq. (A8) are noteworthy. First, the dependence on  $z$  and  $z'$  is separable. Second, the notation used emphasizes the fact that in this paper we work with a slab of finite (in practice, rather small) thickness, for which the spectrum of levels for motion normal to the surface is *discrete*. Third, whereas the sum over the index  $l$  runs over occupied energy levels only (we have denoted by  $l_M$  the highest occupied level), the sum over the index  $l'$  runs over both occupied and unoccupied levels. In practice the upper limit of the latter sum (denoted by  $l'_M$  in Sec. II) is increased until the physical results converge to a desired accuracy.

We note that an alternative representation for  $\chi^{(0)}(q_{\parallel}, \omega | z, z')$  can be obtained by expressing the infinite sum over  $l'$  in terms of the outgoing and incoming Green's functions associated with the single-particle Hamiltonian of Eq. (A7).<sup>29,42</sup> The advantage of such representation is that it involves a sum over occupied levels only. However, for the applications considered in the present

In the jellium model for the periodic background the effective potential depends only on the coordinate normal to the surface, i.e.,  $V_{\text{eff}}(\mathbf{x}) = V_{\text{eff}}(z)$ . Hence, the motion of an electron in the plane of the surface [the plane  $(\mathbf{x}, \mathbf{y})$ ] completely decouples from its motion along the  $z$  axis, and we have

$$\psi_v(\mathbf{x}) = \frac{1}{A^{1/2}} e^{i\mathbf{k}_{\parallel} \cdot \mathbf{x}_{\parallel}} \phi_l(z), \quad (\text{A5})$$

and

$$E_v = \frac{\hbar^2 k_{\parallel}^2}{2m} + \epsilon_l, \quad (\text{A6})$$

where the wave functions  $\phi_l(z)$  and energy eigenvalues  $\epsilon_l$  are the solutions of the one-dimensional equation

$$\left[ -\frac{\hbar^2}{2m} \frac{d^2}{dz^2} + V_{\text{eff}}(z) \right] \phi_l(z) = \epsilon_l \phi_l(z), \quad (\text{A7})$$

with  $l = 1, 2, 3, \dots$ . We note that the  $\{\phi_l(z)\}$  are real.

In the jellium model we can introduce the reduced response function  $\chi^{(0)}(q_{\parallel}, \omega | z, z')$ , defined by an equation of the form of Eq. (2.7). Making use of Eqs. (A5) and (A6) in Eq. (A1) we are led to the result

$$\chi^{(0)}(q_{\parallel}, \omega | z, z') = \sum_{l=1}^{l_M} \sum_{l'=1}^{\infty} F_{ll'}(q_{\parallel}, \omega) \phi_l(z) \phi_{l'}(z) \phi_l(z') \phi_{l'}(z'), \quad (\text{A8})$$

where we have made the definition

work the number of unoccupied levels required is not exceedingly large. Furthermore, in the representation (2.19) for the wave functions  $\phi_l(z)$  it is straightforward to obtain any number of unoccupied states once the effective potential  $V_{\text{eff}}(z)$  has been obtained. Thus we adopt Eq. (A8) on account of its formal simplicity.

We replace the sum over  $\mathbf{k}_{\parallel}$  in Eq. (A9) by an integral by the usual prescription

$$\frac{1}{A} \sum_{\mathbf{k}_{\parallel}} \rightarrow \int \frac{d^2 k_{\parallel}}{(2\pi)^2} = \frac{1}{(2\pi)^2} \int_0^{\infty} dk_{\parallel} k_{\parallel} \int_0^{2\pi} d\theta. \quad (\text{A11})$$

With the change of variables  $u = e^{i\theta}$ , and carrying out a contour integral over the unit circle we can show the result that

$$\int_0^{2\pi} d\theta \frac{1}{\alpha \cos \theta + \beta \pm i\eta} = \mp \frac{2\pi i}{[\alpha^2 - (\beta \pm i\eta)^2]^{1/2}}, \quad (\text{A12})$$

where  $\alpha$  and  $\beta$  are real and we take the branch cut of the complex square root along the negative real axis. Making use of Eqs. (A11) and (A12) in (A9) we are left with the evaluation of a one-dimensional integral over  $k_{\parallel}$  which turns out to be elementary. We thus obtain the following explicit result for the electron-hole pair kernel (A9) for  $l \leq l_M, l' \leq \infty$ :

$$F_{II'}(q_{\parallel}, \omega) = -\frac{m^2}{\pi \hbar^3 q_{\parallel}^2} \left[ 2a_{II'}(q_{\parallel}) + i \left[ \frac{\hbar^2}{m^2} q_{\parallel}^2 k_l^2 - [a_{II'}(q_{\parallel}) - \omega - i\eta]^2 \right]^{1/2} - i \left[ \frac{\hbar^2}{m^2} q_{\parallel}^2 k_l^2 - [a_{II'}(q_{\parallel}) + \omega + i\eta]^2 \right]^{1/2} \right], \quad (\text{A13})$$

where we have made the definition

$$k_l = \left[ \frac{2m}{\hbar^2} (E_F - \epsilon_l) \right]^{1/2}. \quad (\text{A14})$$

We note that in the derivation of Eq. (A13) we have not required that  $\eta$  be infinitesimally small, as it indeed is in the collisionless regime considered in this paper. Now, a finite value of  $\eta$  cannot by itself be associated with collisional damping. In order to incorporate collisions in a conserving approximation, one could adapt to the present problem the relatively simple relaxation-time approximation recently used by Yi and Quinn<sup>43</sup> in the case of a quasi-two-dimensional electron system.

Equations (A8) and (A13) give the result for the electron-hole bubble for a jellium slab used in Ref. 22. In the present paper what we need is the static limit of Eq. (A13). Taking the limits  $\eta \rightarrow 0^+$ ,  $\omega \rightarrow 0$  [recall that the branch cut of the square roots in Eq. (A13) is taken on the negative real axis], and introducing the definition

$$F_{II'}(q_{\parallel}) \equiv F_{II'}(q_{\parallel}, \omega=0), \quad (\text{A15})$$

we have, for  $|a_{II'}(q_{\parallel})| < (\hbar q_{\parallel}/m)k_l$ ,

$$F_{II'}(q_{\parallel}) = -\frac{2m^2}{\pi \hbar^3 q_{\parallel}^2} a_{II'}(q_{\parallel}), \quad (\text{A16a})$$

and, for  $|a_{II'}(q_{\parallel})| > (\hbar q_{\parallel}/m)k_l$ ,

$$F_{II'}(q_{\parallel}) = -\frac{2m^2}{\pi \hbar^3 q_{\parallel}^2} \left[ a_{II'}(q_{\parallel}) - \text{sgn}[a_{II'}(q_{\parallel})] \left[ a_{II'}^2(q_{\parallel}) - \frac{\hbar^2}{m^2} q_{\parallel}^2 k_l^2 \right]^{1/2} \right], \quad (\text{A16b})$$

where  $\text{sgn}x = +1$  for  $x > 0$  and  $-1$  for  $x < 0$ .

<sup>1</sup>M. Rasolt and F. Perrot, Phys. Rev. B **28**, 6749 (1983).

<sup>2</sup>R. N. Barnett, R. G. Barrera, C. L. Cleveland, and U. Landman, Phys. Rev. B **28**, 1667 (1983).

<sup>3</sup>P. Johansson, Solid State Commun. **31**, 591 (1979); P. Johansson and H. Hjelmberg, Surf. Sci. **80**, 171 (1979).

<sup>4</sup>K. W. Lau and W. Kohn, Surf. Sci. **75**, 691 (1978).

<sup>5</sup>A. A. Maradudin and L. J. Sham, in *Proceedings of the International Conference on Lattice Dynamics*, edited by M. Balkanski (Flammarion, Paris, 1977), p. 296; J. F. Dobson and J. H. Rose, J. Phys. C **15**, 7429 (1982).

<sup>6</sup>C. Beatrice and C. Calandra, Phys. Rev. B **28**, 6130 (1983).

<sup>7</sup>D. E. Beck, V. Celli, G. Lo Vecchio, and A. Magnaterra, Nuovo Cimento B **68**, 230 (1970).

<sup>8</sup>D. M. News, Phys. Rev. B **1**, 3304 (1970).

<sup>9</sup>A. Griffin and J. Harris, Can. J. Phys. **54**, 1396 (1976).

<sup>10</sup>G. Gumbs, Phys. Rev. B **27**, 7136 (1983).

<sup>11</sup>G. Gumbs and D. J. W. Geldart, Phys. Rev. B **29**, 5445 (1984).

<sup>12</sup>P. W. Lert and J. H. Weare, J. Phys. C **11**, 1865 (1978).

<sup>13</sup>J. Bardeen, Phys. Rev. **49**, 653 (1936).

<sup>14</sup>R. Fuchs and K. L. Kliewer, Phys. Rev. B **3**, 2270 (1971); R. H. Ritchie and A. L. Marusak, Surf. Sci. **4**, 234 (1966).

<sup>15</sup>N. D. Lang and W. Kohn, Phys. Rev. B **1**, 4555 (1970); **3**, 1215 (1971); and **7**, 3541 (1973).

<sup>16</sup>S. C. Ying, in *Theory of Chemisorption*, edited by J. R. Smith (Springer, Berlin, 1980), p. 3; P. J. Feibelman, Prog. in Surf. Sci. **12**, 287 (1982).

<sup>17</sup>A. G. Eguluz, D. A. Campbell, A. A. Maradudin, and R. F. Wallis, Phys. Rev. B **30**, 5449 (1984).

<sup>18</sup>P. Hohenberg and W. Kohn, Phys. Rev. **136**, B864 (1964); W. Kohn and L. J. Sham, *ibid.* **140**, A1133 (1965).

<sup>19</sup>J. S. Langer and S. H. Vosko, J. Phys. Chem. Solids **12**, 196 (1960).

<sup>20</sup>J. M. Titman and S. H. Kellington, Proc. Phys. Soc. **90**, 499

(1967).

<sup>21</sup>J. F. Dobson and G. H. Harris, Phys. Rev. B **27**, 6542 (1983).

<sup>22</sup>A. G. Eguluz, Phys. Rev. Lett. **51**, 1907 (1983).

<sup>23</sup>O. Gunnarsson and B. I. Lundqvist, Phys. Rev. B **13**, 4274 (1976); D. C. Langreth and J. P. Perdew, *ibid.* **15**, 2884 (1977); D. C. Langreth and M. J. Mehl, *ibid.* **28**, 1809 (1983).

<sup>24</sup>D. A. Campbell, A. G. Eguluz, A. A. Maradudin, and R. F. Wallis (unpublished).

<sup>25</sup>N. D. Lang and A. R. Williams, Phys. Rev. B **18**, 616 (1978); O. Gunnarsson and H. Hjelmberg, Phys. Scr. **11**, 97 (1975).

<sup>26</sup>J. Appelbaum and D. Hamann, Phys. Rev. B **6**, 1122 (1972).

<sup>27</sup>C. O. Almblath, U. von Barth, Z. D. Popovic, and M. J. Stott, Phys. Rev. B **6**, 2250 (1976).

<sup>28</sup>H. Wendel and R. M. Martin, Phys. Rev. B **19**, 5251 (1979); R. M. Martin and K. Kunc, in *Ab Initio Calculation of Phonon Spectra*, edited by J. T. Devreese, V. E. Van Doren, and P. E. Van Camp (Plenum, New York, 1983), p. 49.

<sup>29</sup>A. Zangwill and P. Soven, Phys. Rev. A **21**, 1561 (1980).

<sup>30</sup>See, for example, W. Hanke, Adv. Phys. **27**, 287 (1978).

<sup>31</sup>T. Maniv and H. Metiu, Phys. Rev. B **22**, 4731 (1980); G. E. Korzeniewski, T. Maniv, and H. Metiu, J. Chem. Phys. **76**, 1564 (1982).

<sup>32</sup>Our method has also been successful in approximating the dynamical response of a semi-infinite slab in problems in which the wave-vector transfers are large (the near-surface screening problem) and in which the frequencies involved are below the plasma frequency. See Ref. 22 and A. G. Eguluz, Phys. Rev. B **30**, 4366 (1984).

<sup>33</sup>M. J. Lighthill, *Introduction to Fourier Analysis and Generalized Functions* (Cambridge University Press, Cambridge, 1970).

<sup>34</sup>S. C. Ying, J. R. Smith, and W. Kohn, Phys. Rev. B **11**, 1483 (1975).

<sup>35</sup>E. Zaremba and W. Kohn, Phys. Rev. B **13**, 2270 (1976).

- <sup>36</sup>B. M. Hall, S. Y. Tong, and D. L. Mills, *Phys. Rev. Lett.* **50**, 1277 (1983).
- <sup>37</sup>B. N. J. Persson and N. D. Lang, *Phys. Rev. B* **26**, 5409 (1982); B. N. J. Persson and S. Andersson, *ibid.* **29**, 4382 (1984).
- <sup>38</sup>M. Persson and B. Hellsing, *Phys. Rev. Lett.* **49**, 662 (1982); *Phys. Scr.* **29**, 360 (1984).
- <sup>39</sup>D. C. Langreth, *Phys. Rev. Lett.* **54**, 126 (1985).
- <sup>40</sup>A. Liebsch, *Phys. Rev. Lett.* **54**, 67 (1985).
- <sup>41</sup>S. C. Ying, *Nuovo Cimento B* **23**, 270 (1974); A. G. Eguluz and J. J. Quinn, *Phys. Rev. B* **14** 1347 (1976).
- <sup>42</sup>P. J. Feibelman, *Phys. Rev. B* **12**, 1319 (1975).
- <sup>43</sup>K. S. Yi and J. J. Quinn, *Phys. Rev. B* **27**, 1184 (1983).